pressure, which is one of the most intensive variables in thermodynamics as well as the concentration and temperature,[13–16] can also be used for controlling the intermolecular forces to generate assembled molecules. We found that a poly (vinyl alcohol) (PVA) solution turned into a macrogel or nanoparticle through a simple ultrahigh-pressure process (10,000 atmosphere, 10 min). The morphology of the obtained assembly depended on the PVA concentration, indicating significant inter/intra-molecular hydrogen bonding. Our results demonstrated that ultrahigh-pressure induces hydrogen bonding in water, which is strong enough to maintain microassemblies such as gels and particles.[17,18] Since the interactive potential of molecules is brought out under ultrahigh-pressure, this technology would be applicable to realize the concept for designing assembly molecules proposed by Whitesides and coworkers.[19–21] Furthermore, this methodology leads to the molecular design of pressure-induced molecular assembly, and facilitates nonharmful processes for molecular separation and drug development.

EXPERIMENTAL

Materials

The degree of polymerization of the used PVA (Kuraray, Japan) was 1750. The degree of saponification was 99.8%.

Ultrahigh-Hydrostatic Pressurization

An aqueous PVA solution of predetermined concentration was poured into a plastic bag and was sealed. The bag solution was pressurized using an ultrahigh-pressure machine (hydrostatic pressure). The pressure was set to 1000–10,000 atmospheric pressures, and was processed over the predetermined time period.

Hydrogel Preparation by The Freeze-Thawing Method

An aqueous PVA solution was subjected to five cycles of freeze-thawing, in which the sample was frozen for 12 h at −20 °C, and then thawed for 12 h at 4 °C as one cycle. The mass change of the freeze-thawed sample and the high-pressure processed sample before and after soaking was measured, and the structures of the two gels, both of which had gel ratios over 90%, were compared.

Dynamic Light Scattering Measurement

A 0.5 w/v % PVA solution was high-pressure processed for 10 min at 10,000 atm, and the sample was diluted to an appropriate concentration with ultrapure water, and was subsequently filtered with a 5-μm pore mesh. The particle size was then measured with DLS-7000 (Otsuka Electronics, Japan) using an Ar laser (λ = 488 nm, 75 mW).

Swelling Ratio Measurement

The PVA hydrogel prepared by pressurization was immersed in pure water at room temperature for 10 days and then freeze-dried. The swelling ratio of the PVA hydrogel was calculated as follows:

$$\text{Swelling ratio} = \frac{W_h - W_d}{W_d} \times 100$$

where W_h is the weight of hydrated gel after the dialysis and W_d is the weight of dried gel.

Scanning Electron Microscopy

Observation of PVA assembly was carried out using a scanning electron microscope, S-4700 (Hitachi High Technologies). Specimen for SEM observation was prepared as follows: After a hydrogel was freeze-dried, it was coated with a thin layer of Pt–Pd by the vacuum evaporation technique.

Differential Scanning Calorimetry

DSC measurement was carried out to reveal the melting temperature of PVA assembly. It was carried out at heating rate of 5 °C/min under a constant flow of nitrogen gas.

^{1}H NMR Measurement

The nongelled portion of the pressurized PVA was obtained by the dialysis of the PVA hydrogel. The ^{1}H NMR spectra was obtained by the measurement of the PVA sample dissolved in dimethyl sulfoxide (DMSO-d_6).

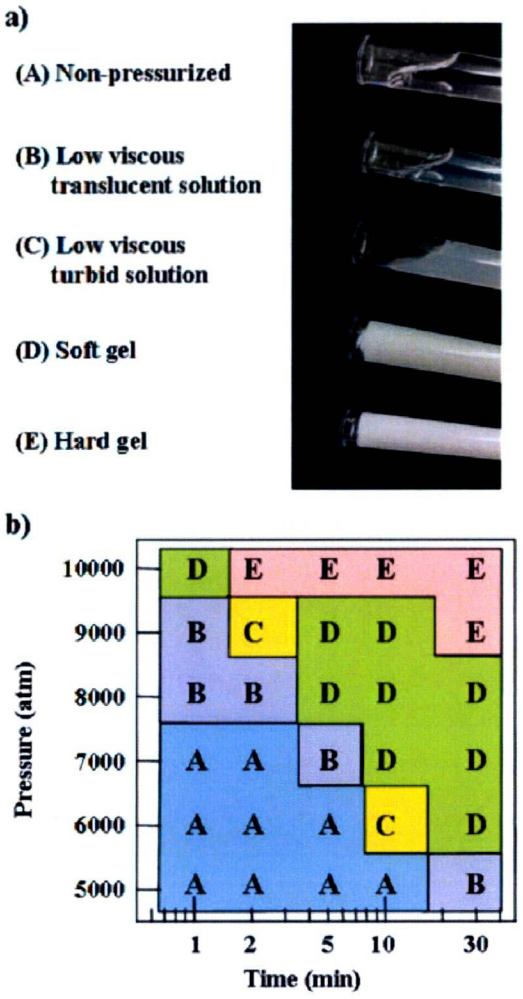

Figure 1. Pressure-induced PVA assembly. (a) Photographs of a 10 w/v% PVA solution pressurized under various conditions: (A) nonpressurized, (B) 7000 atm, 1 min, (C) 9000 atm, 1 min, (D) 7000 atm, 10 min, and (E) 10000 atm, 10 min. (b) Phase (constitutional) diagram of a 5 w/v % PVA solution pressurized under various conditions. The state was decided by visual observation according to the photographs. [Color figure can be viewed in the online issue, which is available at www.interscience.wiley.com.]

RESULTS AND DISCUSSION

PVA Assembly Formed by Pressurization

Aqueous solutions of PVA at 1–20 w/v % concentrations were pressurized hydrostatically under various conditions. Figure 1(a) shows photographs of typical samples of 10 w/v % PVA solutions pressurized at different atmosphere pressure (atm) for 10 min. A translucent solution, the precipitate and hydrogel of PVA was obtained by increasing the pressure, indicating that the assembly of PVA molecules was induced by pressure treatment. The hydrogel was stable in pure water, and the yield (gelation ratio) was 90% or more. It is well-known that PVA solutions transform into hydrogels when the solution was frozen and thawed sequentially several times; this procedure is called the freeze-thawing method. Approximately 10 days is required to form a hydrogel with similar strength as a hydrogel obtained by pressurization for only 10 min. Thus, this simple pressurizing method can be expected to be an energy saving process. The influence of the pressure conditions on the formation of a PVA assembly was examined using a PVA solution of 5 w/v % in detail. Figure 1(b) shows the state diagram of the PVA assembly in a pressure–time plot determined by visual observation according to the photographs shown in Figure 1(a). The translucent solution and hydrogel were acquired by pressure treatment at more than 8000 atm over a very short time (one min). The tendency for gelation of PVA with increasing pressure was observed for each step of pressurization. In addition, at constant pressure, a long period of pressure treatment induced assembly of the PVA, even in the case of only 6000 atm, and the hydrogel was obtained by pressurization for 30 min. Furthermore, DLS measurements of a 10 w/v % solution pressurized under conditions in which a hydrogel was not obtained revealed the formation of PVA nanoassembly and the

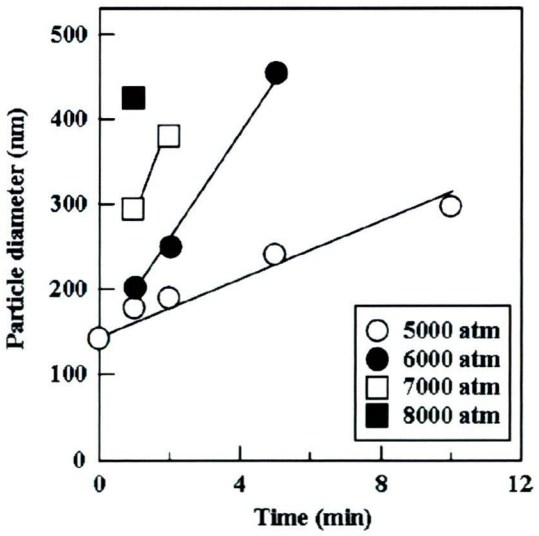

Figure 2. DLS measurements of a 10 w/v % PVA solution pressurized under various conditions.

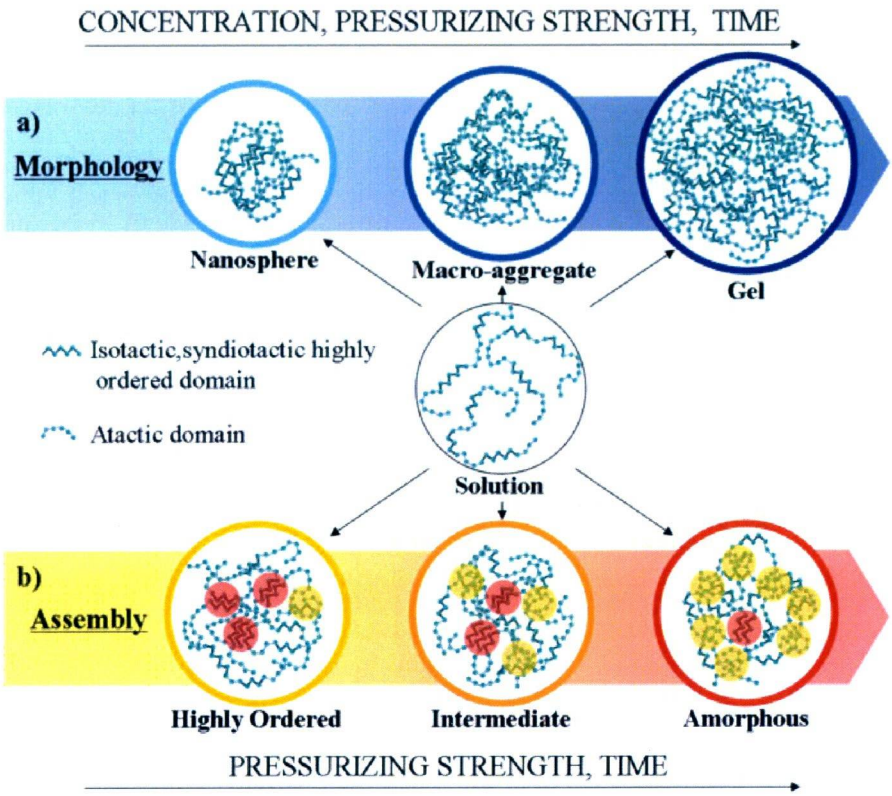

Figure 3. Illustration of the mechanism of hydrogen-bonding polymer assembly induced by ultrahigh-pressurization. (a) Effect of conditional parameters on the morphology of PVA assembly. (b) Effect of secondary structure of PVA on the formation of molecular assembly.

growth of the PVA nanoassembly under prolonged periods of pressure (Fig. 2). From these results, it is clear that the assembly of PVA at nanometer size was promoted under pressure conditions of higher pressure and a longer incubation period, and could be controlled by altering the pressurizing strength and time [Fig. 3(a)].

Characteristics of PVA Assembly Formed By Pressurization

The gelation of a PVA solution at 5, 10, 15, and 20 w/v % concentrations was also achieved by pressurization at 10,000 atm. The swelling ratio of the obtained hydrogel was determined by the starting concentration of the PVA solution, and showed a constant value for all concentrations when they were treated at 10,000 atm for more than 10 min (Fig. 4). On the other hand, the swelling ratio of the obtained hydrogel at 5 min of pressurizing time was inversely proportional to the concentration of the PVA solution (Fig. 5). This result indicates that a tight interaction

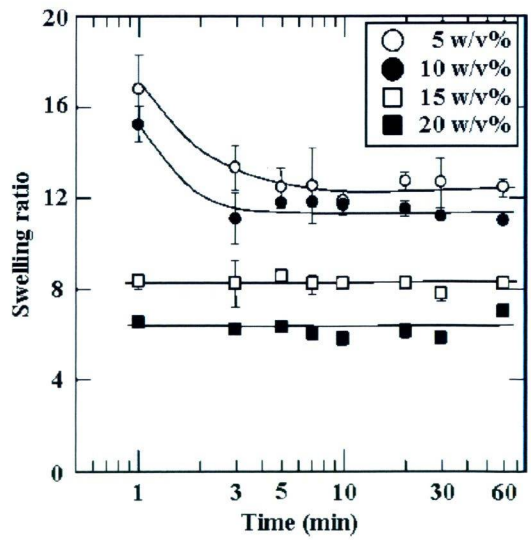

Figure 4. Effect of PVA concentration on swelling ratio of PVA hydrogel formed by pressurization at 10,000 atm for various minutes.

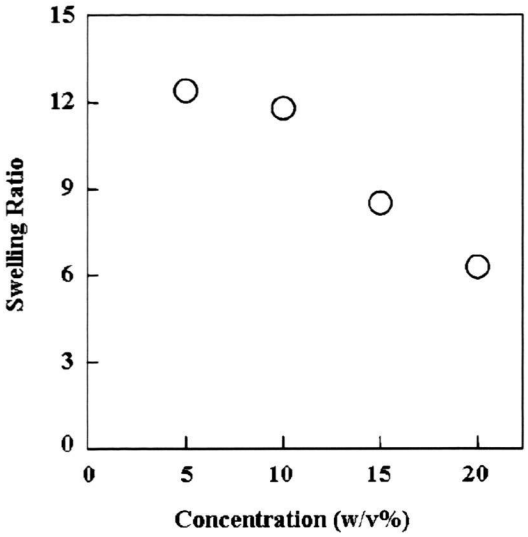

Figure 5. Swelling ratio of PVA hydrogels formed by pressurization at 10,000 atm for 5 min.

between the PVA molecules was formed with increasing the concentration of PVA solution. The interior structure of the PVA hydrogel pressurized at 10,000 atm for 10 min was observed with a SEM (Fig. 6). A mesh-like structure with pores of about 300 nm was observed for the hydrogel obtained by the pressure treatment of a 5 w/v % PVA solution. The mesh-like structures with smaller pores were formed upon increasing the PVA concentration. As the pressure treatment was carried out at 40 °C, no ice crystal was formed.[22] That is, ice crystals did not affect the mesh-like structures formed by the high-pressure process. In contrast, in the case of the freeze-thawing method, the mesh-like structures were formed by the formation of ice crystals. Therefore, a different process of formation between the two methods was suggested.

DSC analysis of the PVA hydrogels let us know the melting temperature of the associated PVA molecules. The relaxation, which occurs at a temperature between 200 and 260 °C, is caused by the melting of the crystalline domains of PVA.[23,24] The increase of intermolecular hydrogen bonding in PVA raises the melting temperature, leading to a high heat resistance.[25] The melting temperature of the PVA hydrogel

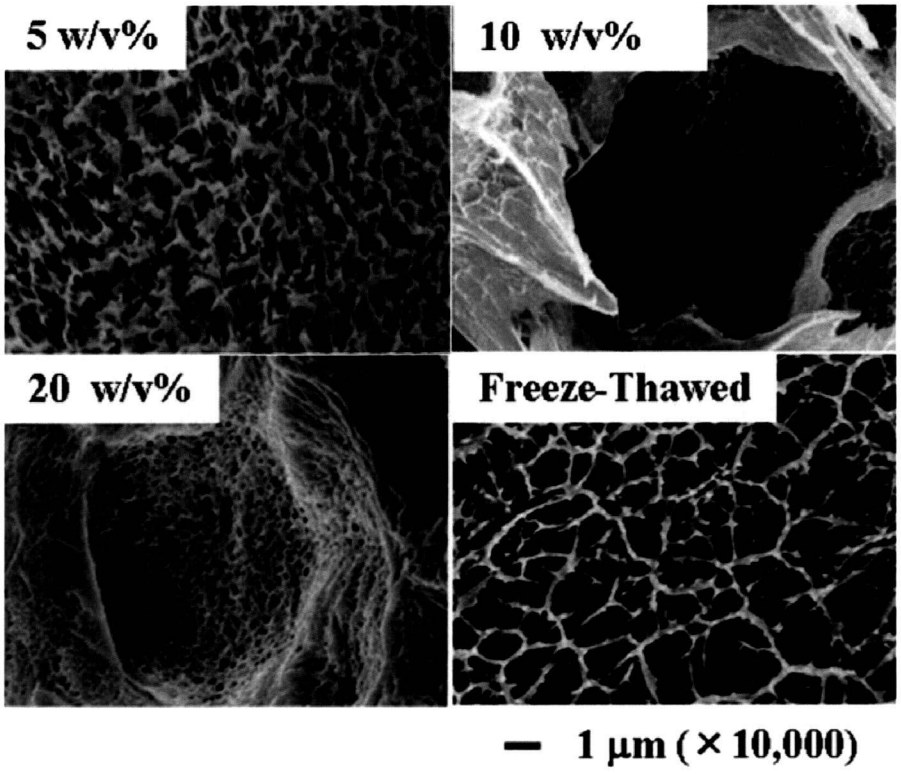

Figure 6. SEM images of PVA hydrogels of 5, 10, and 20 w/v % formed by pressurization at 10,000 atm for 10 min and 5 w/v % PVA hydrogels formed by the freeze-thawing method.

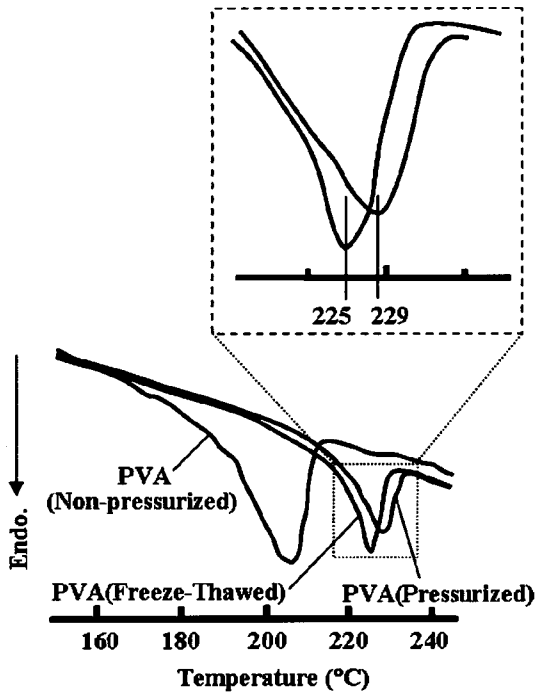

Figure 7. DSC measurements of PVA hydrogels formed by pressure treatment or the freeze-thawing method.

obtained by high-pressure process was higher than that of the hydrogel prepared by the freeze-thawing method (Fig. 7). This result indicates that high-pressure process could form stronger intermolecular interactions in PVA than the freeze-thawing method. Although we need to go into additional details about the thermodynamic stability of the PVA hydrogel obtained by high-pressure process, we have only limited information about it.

Many researchers have examined the self-organization of molecules in an aqueous environment, because the hydrogen bonds and hydrophobic interactions were able to act as a driving force for structure formation.[26–29] The formation and deformation of the hydrogen bonds in an aqueous environment can be controlled by changing the temperature and ionic concentration. The effect of the salt concentration on the high-pressure process of the PVA solution was then examined. When the NaCl concentration was increased, the PVA hydrogel was obtained even at low pressure (around 6000 atm). At over 9000 atm, stable PVA hydrogels were obtained at any salt concentration, and the swelling ratio was almost constant (Fig. 8).

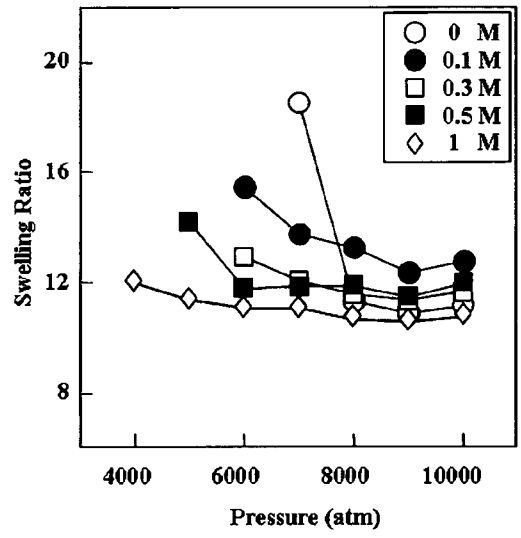

Figure 8. Swelling ratio of 10 w/v% PVA hydrogels formed by pressurization at 10,000 atm for 5 min with various salt concentrations.

When PVA solutions of less than 1 w/v % concentration were treated with pressurization at 10,000 atm, clear and turbid solutions were obtained, as well as in the case of a 10 w/v % PVA solution pressurized under low atmospheric pressure for a short time. The formation of small particles with a diameter of about 200–400 nm was confirmed from SEM observation and DLS measurements (Fig. 9). As a result, it was believed that the formation of intra/inter-molecular hydrogen bonds is the first step in the initial structural formation of PVA, and afterward the size and morphology of the structure is determined in proportion to the concentration of the solution.

The effect of the secondary (atactic, syndiotactic, and isotactic) structure of PVA molecule was observed by the ^{1}H NMR spectra analysis for the nongelled portion of the pressurized PVA solution (Table 1). Short-time pressurizing treatment at

Table 1. NMR Analysis of the Nongelled Portion of the Pressurized PVA Solution

	Tacticity		
	mm	mr	rr
PVA117HC	22.6	47.6	29.8
S-PVA	11.9	49.9	38.2
PVA117HC (20%, 6000 atm, 5 min)	21.4	49.0	29.6
PVA117HC (20%, 6000 atm, 10 min)	33.8	37.7	28.5
PVA117HC (10%, 7000 atm, 5 min)	20.9	48.0	31.1

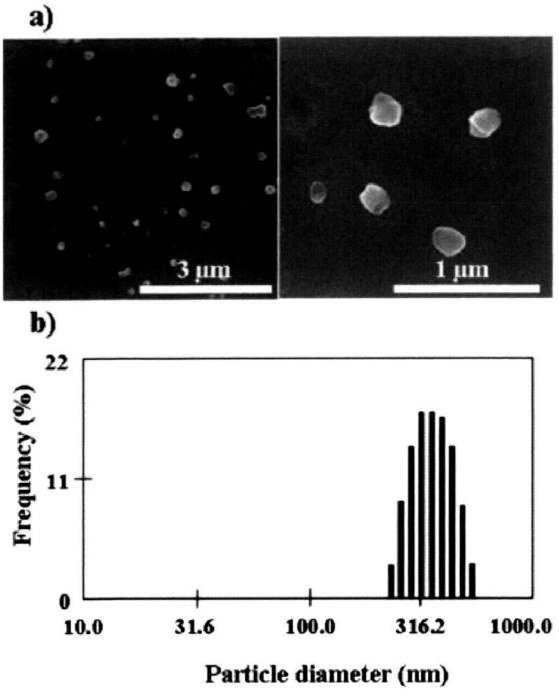

Figure 9. Small aggregates formation of PVA by pressurization. (a and b) SEM images and DLS measurements, respectively, of PVA particles formed by pressurizing a 0.5 w/v % PVA solution at 10,000 atm for 10 min.

6000 atm had no effect on the content of the secondary structure of PVA molecule, whereas after the longer treatment (10 min), the decrease of the atactic portion (mr) of PVA molecule was observed. There was no free PVA after more than 20-min treatment. These results indicated that the atactic PVA was gelled prior to other kinds of the stereostructured PVA, and after prolonged treatment all kinds of stereostructured PVA gelled. These differences of aggregation ability of each stereostructured PVA could be applicable to form the ordered structure by changing treatment time, pressure, and the content of each secondary structures of PVA [Fig. 3(b)].

The High-Ordered Structure of PVA Assembly

The assembly of PVA depended on the strength and period of pressurization and the PVA concentration. It should be noted that molecular assembly is formed through two processes induced by pressurization, which are dehydration and the subsequent formation of hydrogen bonds among inter/intra-molecules. Indeed, it is believed that under pressurized conditions, the hydration shell of the PVA molecules was disrupted, and then hydrogen bonding interactions between the hydroxyl groups of the PVA were formed. Thus, the gelation of PVA was promoted by increasing the pressure. It seems that the reaction could proceed with a long duration of pressurization even at moderate pressures. With regard to the concentration-assembly relationship, monodispersed and nanometer-scale structures were formed by intramolecular interactions under dilute conditions, whereas the macrostructure (larger than mm) was formed by the intermolecular interactions between nanometer-scaled structures which contained molecular entanglements under concentrated conditions. To construct a well-defined molecular assembly, it is necessary to optimize the primary chemical structure of the polymer molecules, and to fabricate molecules with a specific structure by exploiting various interactions. The intermolecular force maintaining the structure of the supramolecular assembly includes van der Waals force, electrostatic interactions, hydrophobic interactions, and hydrogen bonds, etc. The individual interaction energy of a hydrogen bond is small, while if it interacts along the chain direction, hydrogen bond is able to maintain a huge PVA hydrogel by assembling high-molecular weight PVA moieties. The most important factor that influences the structure formation induced by high pressure is the chain length and the secondary structure of the PVA molecule, as well as the temperature, concentration, and ionic concentration. Controlling the factors, it is expected that the ordered structures of molecular assembly can be generated. In a conventional technique, changing the concentration of the solution or a substitution of the solvent makes it difficult to change the molecular-assembly situation gradually. On the other hand, the pressuring conditions can be reversibly controlled and highly controlled operation for molecular assembly by building the interactive part, which works at a different pressure in the molecules. In the case where two or more hydrogen bonding functional groups are present, the control of a higher-order structure can be achieved by pressurizing in a stepwise fashion. We assumed that the secondary structure of PVA is one of the most possible candidates for the factors for obtaining the ordered molecular assembling structure. It is expected that such technology can be applied to build a structure by the manipulating molecular interactions to develop

novel structure in aqueous solution, leading to new science and technology.

CONCLUSIONS

The PVA assembly was simply obtained through an ultrahigh-pressure process. The morphology of PVA assembly depended on the strength and period of pressurization, the PVA concentration, the PVA chain length, and the PVA secondary structure. Under the ultrahigh-pressure, molecular assembly is formed through two processes, which are dehydration and the subsequent formation of hydrogen bonds among inter/intramolecules. Thus, the ultrahigh-pressure process can manipulate molecular interactions. Therefore, it is expected that the novel high-ordered structures based on molecular assembly can be generated by controlling various factors in an ultrahigh-pressure process.

This work was partly supported by Kuraray Co., for their supply of the poly(vinyl alcohol).

REFERENCES AND NOTES

1. Joachim, C.; Gimzewski, J. K.; Aviram, A. Nature 2000, 408, 541–548.
2. Cui, Y.; Lieber, C. M. Science 2001, 291, 851–853.
3. Yokoyama, M.; Miyauchi, M.; Yamada, N.; Okano, T.; Sakurai, Y.; Kataoka, K.; Inoue, S. Cancer Res 1990, 50, 1693–1700.
4. Nishiyama, N.; Kataoka, K. Pharmacol Ther 2006, 112, 630–648.
5. Bong, D. T.; Clark, T. D.; Granja, J. R.; Ghadiri, M. R. Angew Chem Int Ed 2001, 40, 988–1011.
6. Chandler, D. Nature 2005, 437, 640–647.
7. Tanaka, T.; Tasaki, T.; Aoyama, Y. J Am Chem Soc 2002, 124, 12453–12462.
8. Zemb, T. Curr Opin Colloid Interface Sci 2003, 8, 1–4.
9. Lehn, J. M. Proc Natl Acad Sci USA 2002, 99, 4763–4768.
10. Prins, L. J.; De Jong, F.; Timmerman, P.; Reinhoudt, D. N. Nature 2000, 408, 181–184.
11. Barth, J. V.; Weckesser, J.; Lin, N.; Dmitriev, A.; Kern, K. Appl Phys A: Mater Sci Process 2003, 76, 645–652.
12. Balzani, V.; Credi, A.; Raymo, F. M.; Stoddart, J. F. Angew Chem Int Ed 2000, 39, 3348–3391.
13. Mozhaev, V. V.; Heremans, K.; Frank, J.; Masson, P.; Balny, C. Proteins: Struct Funct Genet 1996, 24, 81–91.
14. Kunugi, S.; Yoshida, D.; Kiminami, H. Colloid Polym Sci 2001, 279, 1139–1143.
15. Otero, L.; Sanz, P. D. J Food Sci 2003, 68, 2523–2528.
16. Kalichevsky-Dong, M. T.; Ablett, S.; Lillford, P. J.; Knorr, D. Int J Food Sci Technol 2000, 35, 163–172.
17. Kunugi, S.; Takano, K.; Tanaka, N.; Suwa, K.; Akashi, M. Macromolecules 1997, 30, 4499–4501.
18. Seto, Y.; Kameyama, K.; Tanaka, N.; Kunugi, S.; Yamamoto, K.; Akashi, M. Colloid Polym Sci 2003, 281, 690–694.
19. Bowden, N.; Terfort, A.; Carbeck, J.; Whitesides, G. M. Science 1997, 276, 233–235.
20. Breen, T. L.; Tien, J.; Oliver, S. R. J.; Hadzic, T.; Whitesides, G. M. Science 1999, 284, 948–951.
21. Whitesides, G. M.; Crzybowski, B. Science 2002, 295, 2418–2421.
22. Chou, I. M.; Blank, J. G.; Goncharov, A. F.; Mao, H. K.; Hemley, R. J. Science 1998, 281, 809–812.
23. Nugent, M. J. D.; Higginbotham, C. L. Eur J Pharm Biopharm 2007, 67, 377–386.
24. Hassan, C. M.; Ward, J. H.; Peppas, N. A. Polymer 2000, 41, 6729–6739.
25. Nagara, Y.; Nakano, T.; Okamoto, Y.; Gotoh, Y.; Nagura, M. Polymer 2001, 42, 9679–9686.
26. Arnaud, A.; Belleney, J.; Boue, F.; Bouteiller, L.; Carrot, G.; Wintgens, V. Angew Chem Int Ed 2004, 43, 1718–1721.
27. Kim, C.; Lee, S. J.; Lee, I. H.; Kim, K. T.; Song, H. H.; Jeon, H. J. Chem Mater 2003, 15, 3638–3642.
28. Kawasaki, T.; Tokuhiro, M.; Kimizuka, N.; Kunitake, T. J Am Chem Soc 2001, 123, 6792–6800.
29. Roy, S.; Dey, J. Langmuir 2003, 19, 9625–9629.

Cell removal with supercritical carbon dioxide for acellular artificial tissue

K. Sawada,[1]* D. Terada,[2] T. Yamaoka,[3] S. Kitamura[3] and T. Fujisato[2]

[1]*Department of Integrated Life, Osaka-Seikei College, 3-10-62, Aikawa Higashiyodogawa-ku, Osaka, 533-0007, Japan*
[2]*Department of Biomedical Engineering, Osaka Institute of Technology, 5-16-1 Omiya, Asahi-ku, Osaka, 535-8585, Japan*
[3]*National Cardiovascular Center, 5-7-1 Fujishiro-dai, Suita, Osaka 565-8565, Japan*

Abstract

BACKGROUND: The objective of this work was to decellularize artificial tissue without using surfactant solutions. For this purpose, supercritical carbon dioxide was used as the extraction medium.

RESULTS: Supercritical carbon dioxide containing a small amount of entrainer was a suitable medium to extract both cell nuclei and cell membranes from artificial tissue. Under gentle extraction conditions (15 MPa, 37 °C), cell nuclei were satisfactorily extracted from tissue within 1 h. In contrast, the efficiency of phospholipid removal depended strongly on the transfer rate of carbon dioxide in the interior of the tissue. Mechanical strength of tissue was not decreased even with prolonged treatment.

CONCLUSION: Acellular artificial tissues could be prepared quickly by treatment with a carbon dioxide/entrainer system. The prepared acellular tissue could be obtained in absolutely dry condition. This is advantageous from the viewpoint of long-term preservation without putrefaction and contamination.

Keywords: supercritical carbon dioxide; extraction; decellularization; aorta

INTRODUCTION

In recent years, the regeneration of diseased heart valves by implantation of artificial or animal alternatives has been investigated extensively.[1–5] To accomplish complete tissue regeneration, several problems need to be overcome. For example, acute rejection of the implanted graft must be prevented. The graft must be gradually degraded without losing apparent mechanical strength, and gradually replaced with regenerated recipient tissue after implantation. Furthermore, the recipient's cells should penetrate effectively into the graft. Heart valve replacements are currently performed using synthetic biodegradable polymers such as polylactic acid and polyglycolic acid.[6–9] However, complete reproduction of the heart valves using these synthetic polymers is very difficult because of the complicated structure of the valves. In addition, the mechanical properties of the synthetic polymers, which are used to make long-standing implants, are not equivalent to those of native tissues.

In contrast, replacements of diseased heart valves with healthy valves from animals have been reported recently; the replaced heart valve is markedly more durable than valves made from synthetic polymers. However, strict evaluation of safety for the recipient is necessary. The most important factor to be evaluated is the extent of removal of donor cells, because residual donor cells are the major cause of rejection. Various decellularization methods have been proposed to remove these cells.[10–13] An example of these methods is the use of surfactants, such as SDS and TritonX-100.[14–20] SDS and Triton X-100, which are potent reducers of surface tension, show strong detergent properties and consequently the cells in the tissue appear to be effectively washed out. However, complete removal of toxic surfactants from the tissue is difficult even after repeated rinsing, since they show high affinity to the extracellular matrix. In addition, cross-linking of tissue with a suitable aldehyde is generally performed after surfactant treatment to maintain the mechanical properties of the tissue. However, this process is thought to be related to calcification of the tissue after implantation. Alternative decellularization methods that do not involve the use of chemicals must be effective in overcoming these problems.

In a previous study, a decellularization process for porcine tissue was developed using ultrahigh pressure

* Correspondence to: K. Sawada, Department of Integrated Life, Osaka-Seikei College, 3-10-62, Aikawa Higashiyodogawa-ku, Osaka, 533-0007, Japan
E-mail: sawada-k@osaka-seikei.ac.jp
Contract/grant sponsor: National Natural Science Foundation of China; contract/grant number: 20676043
Contract/grant sponsor: Science and Technology Project of Guangdong Province; contract/grant number: 2006A10602003; 2007B11000005
Contract/grant sponsor: Science and Technology Project of Guangzhou; contract/grant number: 2007Z3-E4101
Contract/grant sponsor: Open Project Program of the State Key Laboratory of Catalysis, Dalian Institute of Chemical Physics, Chinese Academy of Sciences; contract/grant number: N-06-06
(Received 10 October 2007; revised version received 18 December 2007; accepted 19 December 2007)
Published online 14 March 2008; DOI: 10.1002/jctb.1899

 J Chem Technol Biotechnol 0268–2575/2008/$30.00

in aqueous solutions.[21] The use of ultrahigh pressure and subsequent rinsing in aqueous solution showed excellent effectiveness in removing the cells without the use of surfactants or other chemicals. In addition, inactivation of retrovirus was also attained without losing the mechanical strength of the tissue. However, phospholipids were not removed from the cell membrane, although the cell nuclei were completely removed. To remove the remaining phospholipid from the tissue, additional rinsing in alcohol for 3 days was necessary. Furthermore, more than 2 weeks was necessary to complete this process. Because of the prolonged treatment and the need for several steps when this method is used, a simpler decellularization procedure is desirable.

In this study, a novel method for the decellularization of tissue that did not require a long period for completion and did not involve multiple steps was investigated. The process used the supercritical fluid extraction technique. Supercritical fluids are used in a variety of industrial fields. One of the attractive characteristics of supercritical fluids is their transport coefficients. For example, the diffusion coefficient of a supercritical fluid is intermediate between those of gases and liquids. On the other hand, the viscosity of a supercritical fluid is equivalent to that of a gas. Consequently, a supercritical fluid has a high transfer rate and high permeability. Furthermore, these values can be changed continuously by varying the temperature and pressure. Thus far, supercritical fluids have been applied in the selective extraction of valuable materials in fields such as pharmacy and food science.[22,23]

The strategy for the decellularization of tissue was to use supercritical fluid extraction of the cells by varying the permittivity of the medium. This method has the potential to extract cells effectively with a single extraction medium by controlling the operating pressure. In this study, carbon dioxide was selected as the extraction medium and porcine aorta as the tissue. Because carbon dioxide has moderate critical conditions ($T_C = 32\,^{\circ}C$, $P_C = 7.38\,MPa$), the mechanical properties of the tissue are unlikely to be lost during treatment under supercritical conditions. In addition, carbon dioxide in the tissue will return to the gaseous state after treatment and will naturally diffuse toward the outside of the tissue. As a result, there is no possibility of chemicals remaining in the tissue. Thus, decellularized tissue prepared by this method will be safe for the recipient after implantation.

This study was a fundamental investigation to collect basic information for future application of the process to other organs, such as heart valves and trachea.

EXPERIMENTAL

Materials

Porcine aorta was isolated from a Clawn miniature pig obtained from Japan Faram Co. Ltd. Before treatment of the aorta with supercritical carbon dioxide, moisture on its surface was removed with filter paper. In all experiments, the aorta was cut into 1 g pieces. Pure grade carbon dioxide (>99.9%) was used, purchased from Sumitomo Seika Chemicals Co. Ltd, Japan. If necessary, ethanol was used as an entrainer. Ethanol (SIGMA-ALDRICH Japan K.K., Japan) was of reagent grade and was used after drying with a 3A molecular sieve.

Procedure

Decellularization of porcine aorta was examined using a high-pressure reaction apparatus. Figure 1 is a schematic diagram of the apparatus. The main components of the apparatus include a pressurizing pump, stainless steel vessel, and backpressure regulator. The pressurizing pump (SCF-Get; Jasco Corporation, Japan) supported the flow of carbon dioxide at the desired rate. The stainless steel vessel had a total volume of 50 cm^3 and a diameter of 3 cm. The vessel was placed in a water bath to control the treatment temperature. The contents of the vessel could be stirred with a Teflon-coated bar driven by an outside magnet. The backpressure regulator (Jasco Corporation) was a computer-controlled machine and was able to release carbon dioxide at the desired flow rate for the desired period. In this study, the releasing pressure was strictly controlled to evaluate the effect of the mass transfer rate of the fluid.

Liquid carbon dioxide from a cylinder was compressed with a pressurizing pump and made to flow into the reaction vessel until the pressure reached the desired value. When an entrainer was needed, excess ethanol (15 mL) was preloaded in the bottom of the vessel. Under the supercritical condition, the ethanol at the bottom of the vessel will dissolve in the upper phase until the carbon dioxide is saturated with ethanol. In all experiments, the aorta was fixed to the upper side of the vessel to prevent direct contact with ethanol. Consequently, in the supercritical condition, the aorta would be surrounded with supercritical carbon dioxide alone or with a mixture of supercritical carbon dioxide and ethanol fluid. Unless otherwise noted, the operating temperature was fixed at 37 °C.

Decellularization was evaluated by hematoxylin–eosin (HE) staining and quantitative analysis of phospholipids. Phospholipid was assayed using the combined enzymatic method reported by Takayama

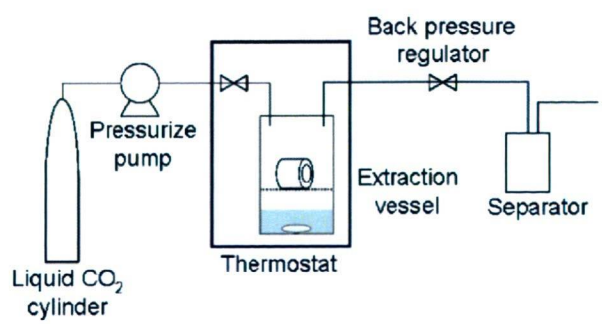

Figure 1. Schematic diagram of the experimental apparatus.

et al.[24] This evaluation method detects phospholipid selectively. To evaluate the mechanical strength of the porcine aorta, tensile strength was evaluated before and after treatment using a Tensilon RTC-1150A (Orientec Co. Ltd, Japan) tensile tester.

RESULTS AND DISCUSSION

Evaluation of decellularization

For evaluating the decellularization of tissues,[25–27] the following two factors are generally recognized as important for the safety of the recipient. The first is the evaluation of the degree of removal of cell nuclei. Because residual donor cell nuclei cause serious rejection, they must be removed as completely as possible. The second factor that should be evaluated is the extent of removal of phospholipid. Phospholipid is the main ingredient of cell membranes and the nuclear membrane. The residue of donor phospholipid is thought to cause gradual deposition of calcium phosphate. As a result, calcification of the tissue may occur. To confirm the decellularization of tissue in this study, residual cell nuclei were evaluated by tissue staining and residual phospholipid by chemical analysis.

Figure 2 summarizes HE staining of porcine aorta treated with supercritical carbon dioxide. A preliminary study confirmed that the degree of cell removal evaluated by HE staining completely agreed with the results obtained by spectrophotometric analysis of DNA. As shown in Fig. 2, the aorta that had been treated with supercritical carbon dioxide only (Fig. 2(b)) was microscopically similar to the native tissue (Fig. 2(a)). Similar results were obtained when the treatment temperature and pressure were varied. Cell nuclei, which have high polarity, seem not to dissolve in non-polar carbon dioxide. On the other hand, supercritical carbon dioxide that contained ethanol was able to extract cell nuclei. As shown in Fig. 2(c) and (d), cell nuclei in the tissue were completely removed from the extracellular matrix. Cell nuclei, which did not dissolve in either carbon dioxide or ethanol, appeared to be effectively solubilized in mixed fluid under the supercritical condition. More remarkable was the decellularization that was attained after a short period of treatment. Figure 2(d) demonstrates that cell nuclei were removed within 15 min when the supercritical carbon dioxide/ethanol system was used. Compared with an aqueous detergent system, the high diffusion coefficient and low viscosity of supercritical fluid will enable rapid access of the fluid into the extracellular matrix. As a result, rapid extraction of cell nuclei can be attained with this system. Because complete decellularization with other techniques is generally performed on a daily basis, supercritical fluid extraction for the same purpose can markedly shorten treatment time. These results show that cell nuclei can easily be removed in a short time without using chemicals such as surfactants and enzymes. A method for quantitative analysis of cell nuclei in supercritical carbon dioxide is not yet established. Future investigations of methods for evaluating the solubility of cell nuclei in supercritical carbon dioxide would be necessary to confirm the observations made in this study.

Figure 3 shows the variation in the percentage of residual phospholipids in the tissue after treatment with supercritical carbon dioxide/ethanol using a batch system. In this case, the operating pressure was fixed at 30 MPa. For comparison, data obtained from a similar system that did not contain ethanol are also shown. As

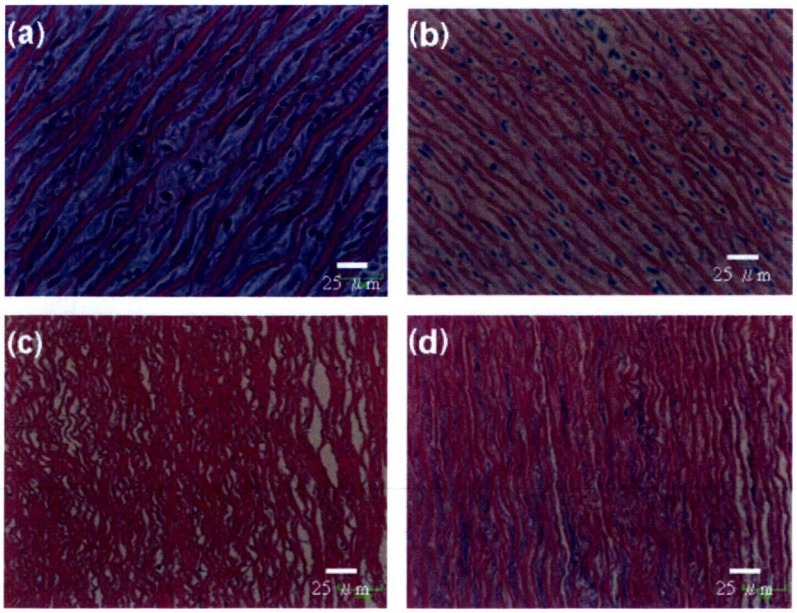

Figure 2. Hematoxylin-Eosin staining of porcine aorta treated in supercritical carbon dioxide. (Batch system): (a) native aorta; (b) aorta treated with supercritical carbon dioxide only; (c) aorta treated with supercritical carbon dioxide/ethanol for 1 h; (d) aorta treated with supercritical carbon dioxide/ethanol for 15 min.

described before, residual phospholipid from a donor may cause calcification after implantation. Therefore, complete removal of phospholipid is desirable during the decellularization process. As shown in Fig. 3, in the absence of ethanol, the system had little ability to extract phospholipid. The results showed that neither cell nuclei nor phospholipid appeared to dissolve in carbon dioxide alone, even when the system was in the supercritical condition. On the other hand, inclusion of ethanol in the system had an obvious effect on the extraction of phospholipid; data show that the percentage of residual phospholipid in the tissue decreased with increasing treatment time and reached a plateau. In this experimental condition, extraction of phospholipid could be attained by 30 min of treatment. Mixed supercritical fluid (carbon dioxide/ethanol), which rapidly reached the inside of the tissue, seems to have the potential to solubilize and extract both cell nuclei and phospholipid within a short time. However, complete extraction of phospholipid was not attained. Some phospholipid remained in the tissue even when the treatment was prolonged.

Figure 4 shows the effects of operating pressure on removal of phospholipid from the tissue. Operating time was fixed at 60 min. As shown in Fig. 4, the percentage of residual phospholipid in the tissue decreased with increasing pressure and reached a plateau. Because an increase in pressure results in an increase in solvent power, the solubility of high-polar phospholipid gradually increased with increasing pressure. The data indicate that the solvent power of a supercritical carbon dioxide/ethanol system at about 20 MPa was sufficient to solubilize phospholipid. Further increase in pressure has only an insignificant effect on the solubilization of phospholipid. As shown before, removal of the cell nuclei could also be attained at 20 MPa. From these data, it is concluded that 20 MPa is the threshold pressure for decellularization of tissue with a supercritical carbon dioxide/ethanol system. Unfortunately, residual phospholipid in the tissue did not reach zero. Some phospholipids remained even when the pressure was raised.

These results may be related to the operating system of the apparatus. The data shown in Figs 3 and 4 were obtained in experiments using a batch system. Because adsorption and desorption of solute in this system are

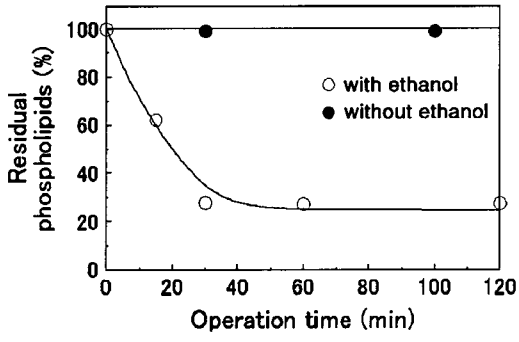

Figure 3. Effect of treatment time on the phospholipid removal from tissue in supercritical carbon dioxide (batch system).

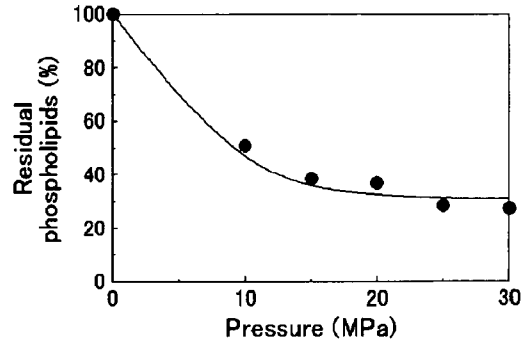

Figure 4. Effect of treatment pressure on the phospholipid removal from tissue in supercritical carbon dioxide (batch system).

in equilibrium with each other, complete removal of phospholipid in a single trial may be difficult. For the complete removal of phospholipid, repetition of the procedure is necessary. However, it is difficult to determine operating times for individual tissues, since tissues differ from each other. In addition, repetition of the operation is not favorable from the perspective of reducing operation time and retaining the mechanical strength of the tissue. In contrast, the use of a system that can control the continuous flow of the fluid may be effective in reducing the amount of residual phospholipids in the tissue. In the following experiments, data were collected from such a system.

Figure 5 shows variations in residual phospholipid in the tissue as a function of treatment time. In this case, the flow rate of the supercritical carbon dioxide/ethanol mixture was 1 mL min^{-1}. Overflowing fluid mixture was captured with a trap through a backpressure regulator. As shown in Fig. 5, phospholipid in the tissue was effectively removed by a short period of treatment. Comparison with the data in Fig. 3 shows that the time to reach a constant percentage of residual phospholipid with this system was shorter than the time required using the batch system. However, some phospholipids remained in the tissue. The amount of residual phospholipids was about 20% of the amount in native tissue and was only slightly different from that in the batch system. Similar data were obtained when the operating pressure was varied. From these data, fluid flow appears not to affect extraction efficiency, but improves extraction velocity.

In order to improve phospholipid removal, further investigation was undertaken taking into consideration the mass transfer rate of mixed fluid in the tissue. It is generally accepted that phospholipids within a tissue must migrate to the surface of the tissue if extraction is to succeed. In this step, the mass transfer rate of the fluid would be closely related to the migration of phospholipids. However, the mass transfer rate of mixed fluid within the tissue under the constant flow condition may be negligible compared with that on the outside. On the other hand, considerable mass transfer of mixed fluid within the tissue would be observed on increasing or decreasing pressure. In the process of increasing the pressure, mixed fluid

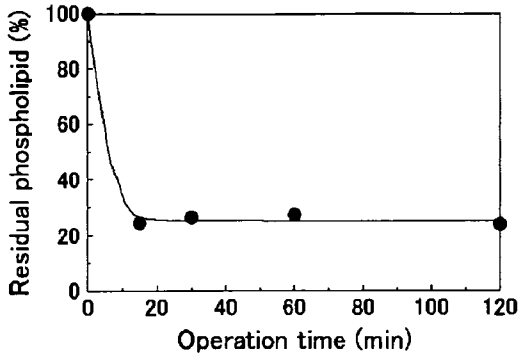

Figure 5. Effect of treatment pressure on the phospholipid removal from tissue in supercritical carbon dioxide (flow system).

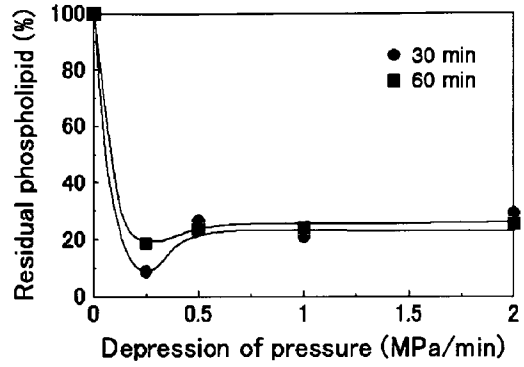

Figure 6. Effect of depression pressure on the phospholipid removal from tissue in supercritical carbon dioxide (flow system).

in the tissue will not move to the outside because the system is closed until the pressure reaches the desired value. In contrast, the process of decreasing the pressure favors the transfer of mixed fluid to the outside through the backpressure regulator. As a result, phospholipids solubilized in the mixed fluid also migrate to the outside of the tissue. In order to evaluate this hypothesis, carbon dioxide in the vessel was gradually released at a strictly controlled flow rate. In this case, pressure was decreased after treatment at constant pressure (30 MPa) for 30 or 60 min.

Figure 6 shows phospholipid removal as a function of pressure depression velocity. It is obvious that pressure depression velocity affects phospholipid removal. The migration velocity of phospholipids in the tissue was also determined at the time of depression of pressure. The data show that the most effective rate of reducing the pressure was 0.25 MPa min^{-1}. Phospholipid removal was lower at a pressure depression velocity of 0.25 MPa min^{-1} than at other rates shown in Fig. 6. A lower pressure depression velocity produces slower variation in the solubility parameter of the mixed fluid. This indicates that phospholipids have considerable opportunity to solubilize in a suitable polar fluid. From the data in Fig. 6, the depression velocity of 0.25 MPa min^{-1} seems to be the best value for both solubilization and migration of phospholipids. However, residual phospholipids did not reach zero throughout the range of depression velocities tested. As described before, continuous pressure depression provides variation in the solubility parameter of the mixed fluid. As a result, some of the phospholipids solubilized in the mixed fluid would be precipitated before migration to the outside of the tissue. Further detailed investigation to determine the best pressure depression velocity may lead to greater efficiency of phospholipid removal in this system.

Evaluation of mechanical properties of tissue

Figure 7 shows stress–strain curves for porcine aorta treated with the supercritical carbon dioxide/ethanol system. The operating pressure was fixed at 35 MPa. As shown in Fig. 7, mixed fluids seem to have no influence on the ultimate breaking strength of

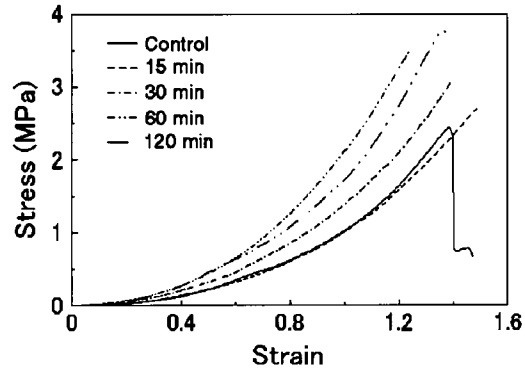

Figure 7. Stress–strain curves of porcine aorta treated in supercritical carbon dioxide (flow system).

the tissue. This suggests that collagen and elastin fibers in the extracellular matrix of the tissue are not broken even if the system is in a high-pressure condition. Because the investigations in this study were performed at a comparatively low temperature and pressure, carbon dioxide in the reaction vessel would not have had enough energy to break the chemical bond of protein fibers in the extracellular matrix. On the other hand, the slope of the curve in Fig. 7 increases with increasing operation time. Prolonging the operation time under the supercritical condition causes hardening of the tissue, which becomes considerable in the high-strain region. This result may be related to tissue dehydration. Because fresh ethanol/carbon dioxide mixture constantly flowed in the reaction vessel for appropriate times, the water content in the tissue decreased with time. As a result, the stereo structure of the protein fibers in the extracellular matrix may have gradually degenerated.

Figure 8 shows the effects of operating pressure on the mechanical strength of porcine aorta. The operation time was fixed at 60 min. The data are similar to those in Fig. 7. The ultimate breaking strength of the tissue was not decreased. On the other hand, an increase in operating pressure causes hardening of the tissue. This result may also be explained in terms of variation in the stereo structure of the protein fibers. An increase in pressure under constant temperature results in an increase in the

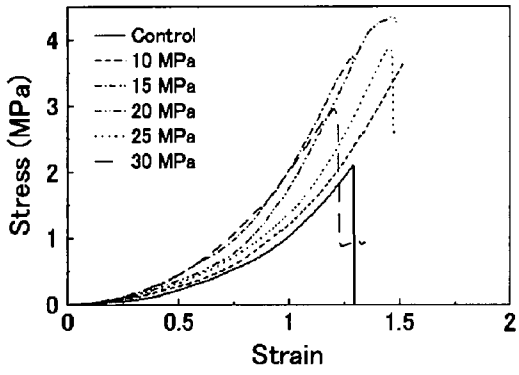

Figure 8. Stress–strain curves of porcine aorta treated in supercritical carbon dioxide (flow system).

density of carbon dioxide. The ethanol content is higher at higher densities of carbon dioxide. As a result, water in the tissue dehydrates easily under the condition of higher carbon dioxide density.

These findings are supported by the data in Fig. 9, which shows the weight variation of the aorta after treatment with supercritical carbon dioxide/ethanol. As shown in the curves identified by circles, the weight of porcine aorta decreased to about 70% that of the native tissue after treatment with only supercritical carbon dioxide/ethanol. The water in the tissue was obviously removed and dissolved in the fluid mixture. However, the weight of the aorta did not recover compared with that of the native tissue even if the aorta was soaked in aqueous solution. Weight recovery was about 90% that of the native weight. This result suggests that treatment with supercritical carbon dioxide/ethanol reduces the possibility of incorporation of water in the inner part of the tissue. Insignificant variation in the stereo structure of the tissue due to dehydration with ethanol may cause slight contraction of the tissue.

These results show that the ethanol in supercritical carbon dioxide causes tissue dehydration. Hardening of the tissue due to dehydration became considerable in the high-strain region. Fortunately, the strain that an organ is subjected to during practice is represented toward the lower end of the abscissa (Figs 7 and 8). In this strain region, differences in hardening due to differences in operating conditions will be negligible. In addition, the ultimate breaking strength of the tissue was equivalent to that of the native standard. The most important role of decellularized tissue is to retain mechanical strength as a scaffold. Tissue prepared in this study had satisfactory characteristics in this respect. In order to investigate the strength of tissue in detail, *in vivo* evaluation in a long-standing implantation is necessary.

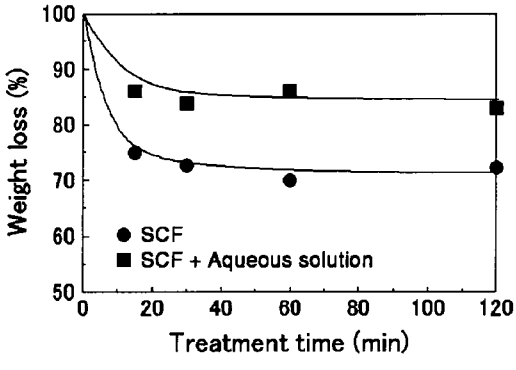

Figure 9. Comparison of weight recovery of porcine aorta before and after the treatment in supercritical carbon dioxide.

CONCLUSIONS

Supercritical carbon dioxide that contained a small amount of ethanol was used as an extraction medium to remove the cells from artificial tissue. The cell nucleus and cell membrane in the tissue could be effectively removed within 20 min under mild conditions (15 MPa, 37 °C). No decrease was observed in the mechanical strength of the tissue because of treatment under the supercritical condition.

The safety level of the recipient is high if the decellularized tissue is processed using supercritical carbon dioxide, because undesirable chemicals such as surfactants and aldehydes are not necessary. In addition, decellularized tissue can be obtained in an absolutely dry condition. This means that the decellularized tissue can be preserved semipermanently until use. Further evaluation for pathogens, such as endogenous viruses and prions, would increase the potential of the supercritical fluid extraction method for preparing acellular artificial tissue.

REFERENCES

1 Badylak SF, Kochupura PV, Cohen IS, Doronin SV, Saltman AE, Gilbert TW, *et al.*, The use of extracellular matrix as an inductive scaffold for the partial replacement of functional myocardium. *Cell Transplant* **15**:S29–S40 (2006).

2 Deguchi K, Tsuru K, Hayashi T, Takaishi M, Nagahara M, Nagotani S, *et al.*, Implantation of a new porous gelatin-siloxane hybrid into a brain lesion as a potential scaffold for tissue regeneration. *J Cereb Blood Flow Metab* **26**:1263–1273 (2006).

3 Triolo F and Gridelli B, End-stage organ failure: will regenerative medicine keep its promise? *Cell Transplant* **15**:S3–S10 (2006).

4 Schoen FJ, New frontiers in the pathology and therapy of heart valve disease. *Cardiovasc Pathol* **15**:271–279 (2006).

5 Schoen FJ, Cardiac valves and valvular pathology: update on function, disease, repair, and replacement. *Cardiovasc Pathol* **14**:189–194 (2005).

6 Webb AR, Yang J and Ameer GA, Biodegradable polyester elastomers in tissue engineering. *Expert Opin Biol Ther* **4**:801–812 (2004).

7 Nuttelman CR, Henry SM and Anseth KS, Synthesis and characterization of photocrosslinkable, degradable poly(vinyl alcohol)-based tissue engineering scaffolds. *Biomaterials* **23**:3617–3626 (2002).

8 Stock UA and Mayer JE Jr, Tissue engineering of cardiac valves on the basis of PGA/PLA Co-polymers. *J Long Term Eff Med Implants* **11**:249–260 (2001).

9 Kim WG, Park JK, Park YN, Hwang CM, Jo YH, Min BG, *et al.*, Tissue-engineered heart valve leaflets: an effective method for seeding autologous cells on scaffolds. *Int J Artif Organs* **23**:624–628 (2000).

10 Kasimir MT, Rieder E, Seebacher G, Silberhumer G, Wolner E, Weigel G, *et al.*, Comparison of different decellularization procedures of porcine heart valves. *Int J Artif Organs* **26**:421–427 (2003).
11 Schmidt CE and Baier JM, Acellular vascular tissues: natural biomaterials for tissue repair and tissue engineering. *Biomaterials* **21**:2215–2231 (2000).
12 O'Brien MF, Goldstein S, Walsh S, Black KS, Elkins R and Clarke D, The SynerGraft valve: a new acellular (nonglutaraldehyde-fixed) tissue heart valve for autologous recellularization first experimental studies before clinical implantation. *Semin Thorac Cardiovasc Surg* **11**:194–200 (1999).
13 Allaire E, Bruneval P, Mandet C, Becquemin JP and Michel JB, The immunogenicity of the extracellular matrix in arterial xenografts. *Surgery* **122**:73–81 (1997).
14 Korossis SA, Booth C, Wilcox HE, Watterson KG, Kearney JN, Fisher J, *et al.*, Tissue engineering of cardiac valve prostheses II: biomechanical characterization of decellularized porcine aortic heart valves. *J Heart Valve Dis* **11**:463–471 (2002).
15 Kim WG, Park JK and Lee WY, Tissue-engineered heart valve leaflets: an effective method of obtaining acellularized valve xenografts. *Int J Artif Organs* **25**:791–797 (2002).
16 Booth C, Korossis SA, Wilcox HE, Watterson KG, Kearney JN, Fisher J, *et al.*, Tissue engineering of cardiac valve prostheses I: development and histological characterization of an acellular porcine scaffold. *J Heart Valve Dis* **11**:457–462 (2002).
17 Korossis SA, Wilcox HE, Watterson KG, Kearney JN, Ingham E and Fisher J, In-vitro assessment of the functional performance of the decellularized intact porcine aortic root. *J Heart Valve Dis* **14**:408–421 (2005).
18 Kasimir MT, Weigel G, Sharma J, Rieder E, Seebacher G, Wolner E, *et al.*, The decellularized porcine heart valve matrix in tissue engineering: platelet adhesion and activation. *Thromb Haemost* **94**:562–567 (2005).
19 Meyer SR, Chiu B, Churchill TA, Zhu L, Lakey JR and Ross DB, Comparison of aortic valve allograft decellularization techniques in the rat. *J Biomed Mater Res A* **79**:254–262 (2006).
20 Rieder E, Seebacher G, Kasimir MT, Eichmair E, Winter B, Dekan B, *et al.*, Tissue engineering of heart valves: decellularized porcine and human valve scaffolds differ importantly in residual potential to attract monocytic cells. *Circulation* **111**:2792–2797 (2005).
21 Fujisato T, Kishida A, Funamoto S, Nakatani T and Kitamura S. Jpn Kokai Tokkyo Koho JP 2004–97552.
22 Dean JR and Khundker S, Extraction of pharmaceuticals using pressurised carbon dioxide. *J Pharm Biomed Anal* **15**:875–886 (1997).
23 Reverchon E and De MI, Supercritical fluid extraction and fractionation of natural matter. *J Supercrit Fluid* **38**:146–166 (2006).
24 Takayama M, Itoh S, Nagasaki T and Tanimizu I, A new enzymatic method for determination of serum choline-containing phospholipids. *Clin Chim Acta* **79**:93–98 (1977).
25 Mcfetridge PS, Daniel JW, Bodamyali T, Horrocks M and Chaudhuri JB, Preparation of porcine carotid arteries for vascular tissue engineering applications. *J Biomed Mater Res* **70A**:224–234 (2004).
26 Mertsching H, Schanz J, Walles T, Hofmann M and Knapp WH, Engineering of a vascularized scaffold for artificial tissue and organ generation. *Biomaterials* **26**:6610–6617 (2005).
27 Gilbert TW, Sellaro TL and Badylak SF, Decellularization of tissues and organs. *Biomaterials* **27**:3675–3683 (2006).

ELSEVIER

European Journal of Cardio-thoracic Surgery 34 (2008) 833–838

EUROPEAN JOURNAL OF CARDIO-THORACIC SURGERY

www.elsevier.com/locate/ejcts

Patency rate of the internal thoracic artery to the left anterior descending artery bypass is reduced by competitive flow from the concomitant saphenous vein graft in the left coronary artery

Masashi Kawamura [a], Hiroyuki Nakajima [a,*], Junjiro Kobayashi [a], Toshihiro Funatsu [a], Yoritaka Otsuka [b], Toshikatsu Yagihara [a], Soichiro Kitamura [a]

[a] *Department of Cardiovascular Surgery, National Cardiovascular Center, 5-7-1 Fujishirodai, Suita, Osaka, 565-8565, Japan*
[b] *Department of Cardiology, National Cardiovascular Center, 5-7-1 Fujishirodai, Suita, Osaka, 565-8565, Japan*

Received 20 January 2008; received in revised form 30 June 2008; accepted 11 July 2008; Available online 23 August 2008

Abstract

Objective: In coronary artery bypass grafting (CABG), insufficient bypass flow can be a cause of occlusion or string sign of the internal thoracic artery (ITA) graft. A patent saphenous vein (SV) graft from the ascending aorta can reduce the blood flow through the ITA graft, and may affect its long-term patency. In the present study, we examined the impact of the patent SV graft to the left coronary artery on the long-term patency of the ITA to left anterior descending (LAD) artery bypass. **Methods:** We reviewed the coronary angiograms of 313 patients who had two bypasses to the left coronary artery including 1 in situ ITA to LAD graft between March 1986 and December 2006. Patients who had occlusion of either bypass grafts to the left coronary artery in the early angiography, were excluded. In 64 patients (20.4%), bilateral ITAs were individually anastomosed to the LAD and the second target branch in the left coronary artery (BITA group), while 249 patients (79.6%) had the ITA to LAD bypass and the SV graft to the second target branch in the left coronary artery (ITA/SV group). The mean follow-up period was 6.8 ± 4.9 years. **Results:** The cumulative patency rate of ITA-LAD bypasses at 10 years was 100% in the BITA group and 81.4% in the ITA/SV group. The ITA to LAD bypass was occluded in 14 (5.6%) patients of the ITA/SV group. In the ITA/SV group, the cumulative graft patency rate of the ITA to LAD bypass in patients who had severe (≥76%) native coronary stenosis between the two anastomotic sites was 98.6% at 5 years, and was significantly higher than that of 82.3% in patients without severe stenosis ($p < 0.0001$). **Conclusions:** Long-term patency of the ITA-LAD bypass was affected by the presence of the patent SV graft to the left coronary artery, particularly when the native coronary stenosis between the two anastomotic sites was not severe. Competitive flow from SV graft could play an important role in occlusion of the in-situ arterial graft.

Keywords: Coronary artery bypass grafting; Internal thoracic artery; Saphenous vein graft; Competitive flow; Graft arrangement

1. Introduction

The utilization of an internal thoracic artery (ITA) in coronary artery bypass grafting (CABG) has decreased the operative mortality without increasing the operative complications [1,2]. The ITA to the left anterior descending artery (LAD) in coronary revascularization has been proven to have a superior long-term patency rate [3], and it improves the long-term mortality and morbidity in patients with coronary artery disease [4–8] as compared to use of vein grafts to the LAD.

On the other hand, a current issue regarding the ITA graft is that competitive flow in the ITA graft causes graft occlusion or 'string sign', which represents the narrowing of the artery along its whole length [9]. In previous reports, competitive flow usually arose when native coronary stenosis was not severe, and the patency rate of the ITA graft inversely correlated with severity of native stenosis [10–12].

Recently, various grafts such as ITA, radial artery, gastroepiploic artery, and saphenous vein (SV) graft are applied and designed in various configurations. There are several reports investigating the hemodynamic features of bypass grafts. Kawasuji and colleagues compared the flow capacities of arterial grafts and SV graft and demonstrated that the flow capacity of the in situ ITA graft which represented diastolic blood pressure, was less than that of SV graft, whose proximal anastomosis was placed on the ascending aorta [13]. When the in situ ITA and the SV graft were connected to the same coronary artery system, the patent SV graft may affect the in situ ITA graft. Such

* Corresponding author. Tel.: +81 6 6833 5012; fax: +81 6 6872 7486.
E-mail address: hnakajim@hsp.ncvc.go.jp (H. Nakajima).

1010-7940/$ – see front matter © 2008 European Association for Cardio-Thoracic Surgery. Published by Elsevier B.V. All rights reserved.
doi:10.1016/j.ejcts.2008.07.011

interactions between the SV graft and arterial bypass grafts have not yet been delineated.

The purposes of this study are to examine the effects of the graft material, for the circumflex or diagonal branch on the long-term patency of the ITA to LAD graft, and to delineate the interactive effect between the bypass grafts aiming at establishing appropriate usage of the SV graft and strategy for optimal graft arrangement in CABG.

2. Materials and methods

We reviewed the coronary angiograms of 313 patients who underwent CABG with two bypasses to the left coronary artery including one in situ ITA to LAD graft and early postoperative angiography between March 1986 and December 2006. Of these, 263 were male and 50 female with a mean age of 60.9 ± 8.9 years and a mean follow-up period of 6.8 ± 4.9 years. In our institution, early postoperative coronary and graft angiography was routinely performed about 2 weeks after surgery, except for patients with renal insufficiency, severe atherosclerosis in the aorta or aged more than 80 years. Late coronary angiography was done when patients suffered from chest pain or recurrence of angina pectoris was suspected by electrocardiogram or other clinical symptoms. Late coronary angiograms were carried out on 133 patients in this series (42.5%; 133/313). All coronary angiograms were independently evaluated by cardiologists for coronary artery stenosis and graft patency. Stenoses were grouped as 51–75% and 76–100% by a precise measurement of the minimal luminal diameter and labeled as 'moderate' and 'severe', respectively in the present study.

The in situ ITA graft or the SV graft as an aorto-coronary bypass was exclusively used in an individual fashion for these patients. The patients who did not undergo early postoperative angiography, who had graft occlusion in either of two bypass grafts to the left coronary artery in the early angiography, and who had a gastroepiploic artery, radial artery, sequential or composite graft, were excluded from this study. Patients whose bypass graft to the right coronary artery was occluded, but both bypass grafts to the left coronary artery were patent in early angiography, were included. Ninety-three patients had two bypass grafts in the left coronary artery, and 220 patients had two bypass grafts in the left coronary artery and 1 in the right coronary artery. The second target site in the left coronary artery was the left circumflex artery (LCX) in 270 patients and the diagonal branch (Dx) in 43 patients.

Patients were divided into two groups based on the graft selection for the second target site in the left coronary artery. The BITA group comprised 64 patients in whom the bilateral in situ ITAs were individually anastomosed to the LAD and the second target site (Fig. 1). In the ITA/SV group, 249 patients had a single in situ ITA to LAD and the SV graft to the second target site in the left coronary artery (Fig. 2). Characteristics of both groups are shown in Table 1. In addition, the ITA/SV group was divided into two subgroups based on the severity of native left coronary stenosis between two distal anastomotic sites, which was referred from preoperative coronary angiography (Fig. 3). The subgroup S comprised 189 patients who had

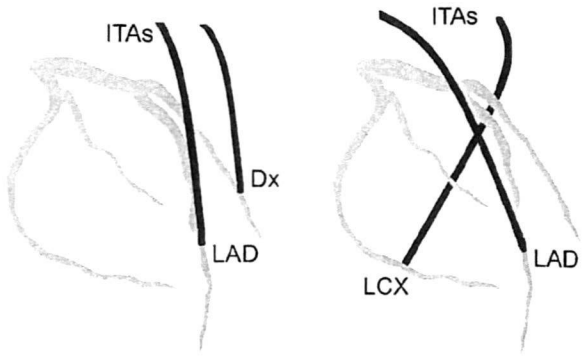

Fig. 1. In the BITA group, bilateral ITAs were individually anastomosed to LAD and the diagonal or circumflex artery. Solid lines indicate the in situ ITA. ITA: internal thoracic artery; LAD: left anterior descending; Dx: diagonal branch; LCX: left circumflex artery.

severe (76–100%) stenosis between two anastomotic sites, while the subgroup M consisted of 60 patients who had moderate (51–75%) or less stenosis between two anastomotic sites. For example, the subgroup S included patients who had severe stenosis at the origin of LAD or circumflex, and the subgroup M included patients with the stenotic lesion localized in the left main trunk.

3. Operative technique

Our current operative technique has been described previously [14]. In brief, our standard technique since 2000 was off-pump CABG without aortic manipulation. Additionally, we preferably use the bilateral in situ ITAs when we place two bypass grafts to relatively large branches in the left coronary artery region in patients without considerable operative risk, such as chronic obstructive pulmonary disease or an advanced age of more than 75 years. A suction-type stabilizer and an apical heart positioner were used for off-pump CABG. The surgical field was maintained by a CO_2 blower and an intracoronary shunt.

Before introduction of an off-pump operation, conventional CABG was performed with ascending aortic and bicaval cannulations. The core temperature was maintained between

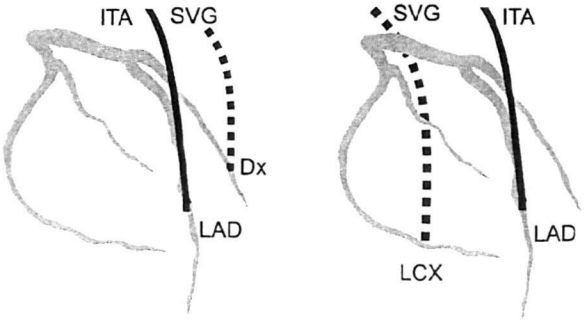

Fig. 2. In the ITA/SV group, an in situ ITA was anastomosed to LAD and the SV graft were anastomosed to Dx or LCX as an aorto-coronary bypass. Solid lines and dash lines indicate ITA and SV graft, respectively. ITA: internal thoracic artery; SV: saphenous vein; LAD: left anterior descending; Dx: diagonal branch; LCX: left circumflex artery.

Table 1
Baseline characteristics in both groups

Characteristics	BITA	ITA/SV	p value
Number of patients	64	249	
Age	59.8 ± 8.7	61.2 ± 8.9	0.30
Follow-up period (years)	4.6 ± 4.4	7.3 ± 4.9	<0.0001
Male/female	59 (92%)/5 (8%)	204 (82%)/45 (18%)	0.046
Hypertension	40 (63%)	117 (47%)	0.03
Hyperlipidemia	38 (59%)	126 (52%)	0.34
Diabetes mellitus	30 (47%)	109 (44%)	0.66
LVEF (%)	50.4 ± 12.2	52.8 ± 13.5	0.26
Operative procedure			
On-pump/off-pump	29 (45%)/35 (55%)	248 (99.6%)/1 (0.4%)	<0.0001
Second target branch in the left coronary artery			
Dx/LCX	6 (9%)/58 (91%)	37 (15%)/212 (85%)	0.26
+ Bypass graft to RCA	19 (30%)	201 (81%)	<0.0001

Mean ± standard deviation. LVEF: left ventricular ejection fraction; CABG: coronary artery bypass grafting; LAD: left anterior descending artery; Dx: diagonal branch; LCX: left circumflex artery; ITA: internal thoracic artery; RCA: right coronary artery; SV: saphenous vein.

32 °C and 34 °C. Intermittent tepid blood cardioplegia was infused antegradely and retrogradely.

The ITA was harvested in either conventional (combined with vein and fascia), semiskeletonized (partially combined with vein) or skeletonized fashion [14]. All distal portions of ITA grafts were greater than 1.5 mm in diameter assessed by insertion of a 1.5-mm flexible probe.

4. Long-term patency rate of the ITA to LAD bypass

We analyzed the long-term patency of the ITA to LAD bypass and examined the effects of graft materials anastomosed to the second target site in the left coronary artery and severity of the native coronary stenosis between two distal anastomotic sites.

5. Statistical analysis

The continuous variables are expressed as mean values ± standard deviations and compared between the two groups by using Wilcoxon rank-sum test. The data of two independent groups were compared using Fisher's exact probability test. The Kaplan–Meier method was used to determine the cumulative graft patency rate and log-rank test was used to compare two groups. The differences in the outcomes were considered statistically significant at a probability value of <0.05.

6. Results

The baseline rate of off-pump CABG in the BITA group was significantly higher than that in the ITA/SV group. Male and hypertensive patients were included in the BITA group with a significantly higher rate as compared to the ITA/SV group. On the other hand, the population of CABG with three distal anastomoses was significantly higher in the ITA/SV group than in the BITA group.

In the ITA/SV group, 14 bypass grafts were occluded during the follow-up period (5.6%; 14/249), whereas, all the ITA-LAD bypasses remained patent in the BITA group. The cumulative patency rate of the ITA-LAD bypass in the ITA/SV group was 94.9% at 5 years and 81.4% at 10 years (Fig. 4).

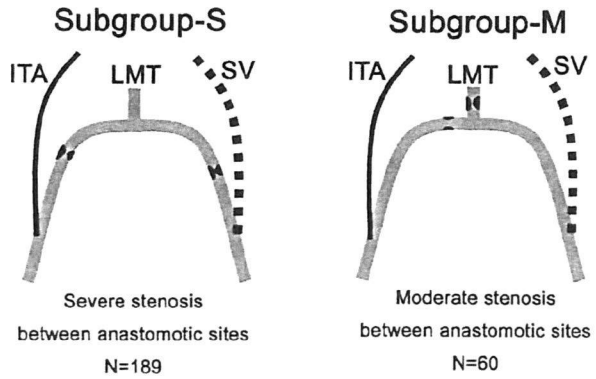

Fig. 3. Patients in the ITA/SV group were divided into two subgroups in regard to severity of the native coronary stenosis between two anastomotic sites (solid line: ITA; dash line: SV graft). ITA: internal thoracic artery; SV: saphenous vein; LMT: left main trunk.

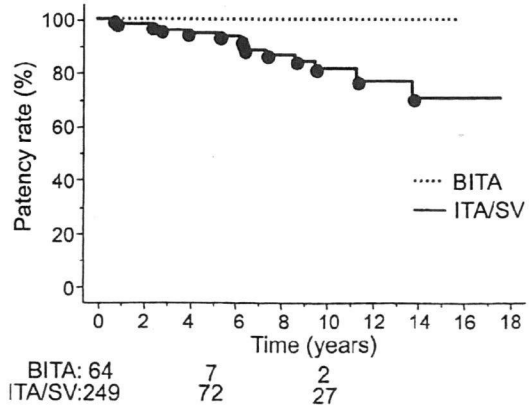

Fig. 4. The cumulative patency rate of the ITA to LAD bypass grafts. The cumulative patency rates at 10 years were 100% in the BITA group and 81.4% in the ITA/SV group. Number at risk is described below the x-axis.

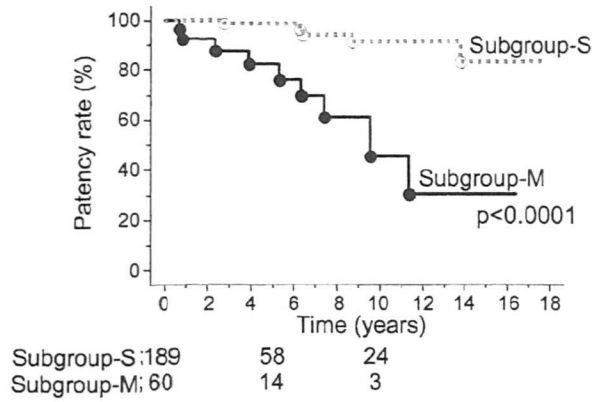

Fig. 5. The cumulative patency of the ITA to LAD bypass grafts. The cumulative patency rates at 10 years were 91.2% in the subgroup S and 45.6% in the subgroup M ($p < 0.0001$). Number at risk is described below the x-axis.

In a comparison of two subgroups of the ITA/SV group, the ITA to LAD bypass graft was occluded in five patients of the subgroup S (2.6%; 5/189) and in nine patients of the subgroup M (15%; 9/60). The cumulative patency rate of the ITA to LAD bypass in the subgroup S were 98.6% at 5 years and 91.2% at 10 years, whereas those in the subgroup M were 82.3% at 5 years and 45.6% at 10 years ($p < 0.0001$) (Fig. 5).

The early and late coronary angiograms of 14 patients with occlusions of the ITA to LAD bypass were carefully reviewed. In 4 out of 14 patients, there were no stenoses of the ITA-LAD bypasses in the early angiograms. However, through SV graft injection of the late angiograms, strong bypass flow from SV graft opacified not only the left circumflex artery but also LAD. In addition, the ITA grafts were visualized by retrograde flow and exhibited 'string sign' (Fig. 6).

7. Discussion

Significant differences in hemodynamic characteristics between the ITA graft and the SV graft have been reported.

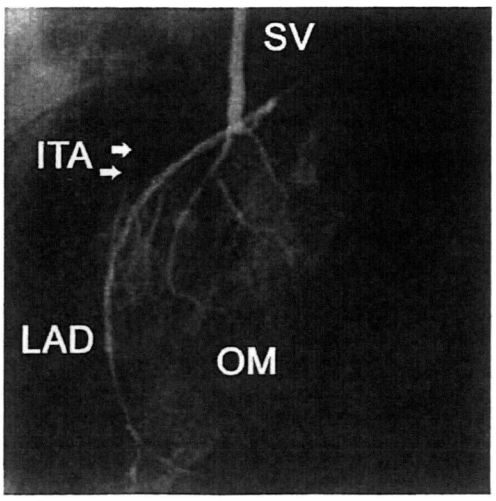

Fig. 6. The distal portion of the ITA graft was visualized by retrograde flow from the SV graft injection (arrows). ITA: internal thoracic artery; SV: saphenous vein; LAD: left anterior descending; OM: obtuse marginal branch.

The SV graft as the aorto-coronary bypass has higher flow capacity than the in situ ITA graft [13] owing to higher blood pressure directly from the ascending aorta and its greater diameter of the SV graft, as compared with those of the in situ ITA graft. Therefore, we presumed that if the patent SV graft to the left coronary artery was present, it might decrease the blood flow in the in situ ITA graft, and diminish its advantage as arterial materials.

In the present study, we attempted to prove the interactive effect between the individual bypass grafts with the different blood source, investigating from a viewpoint of blood flow and patency of arterial grafts. To minimize a bias associated with the bypass grafts and coronary arteries, only patients who had a simple graft arrangement and coronary artery lesions were included. In particular, to eliminate procedural differences, such as on-pump versus off-pump and technical failure, which would be one of the most fundamental biases, patients who had early occlusion of the bypass graft to the left coronary artery were entirely excluded. We focused on the patency of the ITA to LAD bypass, because it is clinically important for survival after CABG.

The results of this study demonstrated that the presence of the patent SV graft anastomosed to the second target site in the left coronary artery reduced the patency rate of the ITA to LAD graft, particularly when the native coronary stenosis between the two distal anastomoses in the left coronary artery was not severe. It was suspected that a mechanism of occlusion of the ITA-LAD bypass was associated with competitive flow from the SV graft by our careful observation of the late coronary angiogram about string of the ITA-LAD bypass.

We previously investigated competitive and reversal flow in sequential and composite arterial grafts, and identified that some specific situations, which were related to two or more coronary branches and arrangement of bypass grafts, significantly increased the incidence of competitive and reversal flow [15]. Moreover, we reported that the graft arrangement with maximized antegrade bypass flow in the arterial grafts played an important role in achieving the advantages of arterial materials and minimizing the incidence of cardiac events after CABG [16]. Since arterial graft occlusion due to insufficient bypass flow mostly occurs within 1 or 2 years [10,16], the long-term prognosis could be jeopardized. We believe that this interactive effect from the SV graft should be avoided as far as possible to achieve the advantage of the arterial graft.

Schmidt and colleagues recommended the use of arterial graft to the second target branch in the left coronary artery because of the superior survival rate [17]. Importance of the circumflex artery over the right coronary artery and inferior patency of the venous graft [18] are considered as primary reasons for the superiority. Results of our study may suggest that interactions of the SV graft on the in situ ITA may be another possible explanation for the superiority of arterial grafting to the second target site in the left coronary artery. We suppose that the use of the SV graft in the right coronary artery region hardly affects the bypass flow in the ITA to LAD graft.

Implications of this study are as follows: patency rate of the ITA to LAD bypass had been believed similar, irrespective

of graft arrangement for the second target branch in the left coronary artery. However, the results of this study strongly suggested that the in situ ITA to LAD bypass only, bilateral ITA grafting, sequential grafting and the composite Y graft to the LAD and the second target branch will provide the higher patency rate of the ITA to LAD bypass than the use of the SV graft to the circumflex or diagonal branch, when the stenosis between the two anastomotic sites in the native left coronary artery is moderate or less. Even in patients unsuitable for bilateral ITA harvest, the avoidance of the SV graft from ascending aorta should be considered.

We suggest that, on the contrary, the in situ ITA to LAD bypass concomitant with the aorto-coronary bypass is suitable when the left coronary and circumflex artery is remarkably large or a large mount of bypass flow is required. The isolated ITA to LAD can be a reasonable option of choice in patients with a localized lesion in the left main trunk. For the concomitant diagonal branch, Dion and colleagues reported excellent long-term patency of sequential grafting with the in situ ITA [19]. According to our previous study, when the circumflex artery is almost occluded and the stenosis in LAD is moderate, the composite Y graft is not recommended, because of the high incidence of competitive flow in the ITA to LAD bypass graft [15]. The severity and location of stenoses in the native coronary artery, the size of the target branch, the distance between and positional relationship of the two target sites, quality of the ITA graft, anticipated flow demand and atherosclerosis of the aorta, etc., should be taken into account for decision of strategy for the second target branch in the left coronary artery.

Limitations of the present study are as follows: first, because this study was retrospective and non-randomized, some differences regarding the characteristics of the BITA and ITA/SV groups were noted. Furthermore, the sample size was considered relatively small. However, the influence of these differences on the late angiographic results could be minimized, because early angiography confirmed that all 313 patients had patent grafts to the left coronary artery, and 133 (42.5%) patients underwent late angiography. Since more than 85% of patients after CABG underwent early angiography in our institution between 1986 and 2006, we considered that the selection bias for angiography was not so significant. Second, although the follow-up period was not enough for development of vein graft disease and ischemia in the left coronary artery region, it would be sufficient for examining correlations between the insufficient flow and arterial graft occlusion, as compared with previous studies [10,16]. In addition, progression of native coronary artery disease during the follow-up period, the length and the location of the stenotic lesion, the size of the circumflex coronary artery could not be taken into account. Moreover, peripheral vascular resistance in the myocardial tissue, and flow demands could also have important roles in the coronary perfusion. However, these factors could not be quantified by reliable methods. The effects of diabetes, hypertension, hyperlipidemia, aspirin and statin medical therapy may be the next concern in the future.

It may be controversial in management of 'string sign', which differs from graft occlusion. Several previous reports documented that the ITA graft with string sign could recover its own lumen when the native coronary artery disease became severe [20,21]. In the statistical analyses of this study, graft occlusion probably associated with string sign was not separated from the other graft occlusion. The reasons for this were as following: (1) contrast medium from the ITA injection did not reach LAD, (2) reversibility is not guaranteed for all ITA grafts presenting string sign, (3) the purpose of this study is to delineate the effect of the abundant blood flow from the SV graft, and (4) it is generally accepted that both graft occlusion and string sign are commonly associated with the abundant native coronary flow.

When we use the combination of the in situ arterial and in situ aorta-coronary venous grafts, it would be necessary to pay attention not to place influence on the patency of the important bypass especially created with the in situ ITA graft. This study is not conclusive in nature and is hypothesis generating only. Further investigations for interactive effects and considerations for the appropriate usage of the SV graft are necessary to establish the strategy for graft arrangement.

References

[1] Grover FL, Johnson RR, Marshall G, Hammermeister KE. Impact of mammary grafts on coronary bypass operative mortality and morbidity. Department of Veteran Affairs Cardiac Surgeons. Ann Thorac Surg 1994; 57:559–69.

[2] Dabel RJ, Goss JR, Maynard C, Aldea GS. The effect of left internal mammary artery utilization on short-term outcomes after coronary revascularization. Ann Thorac Surg 2003;76:464–70.

[3] Lytle BW, Loop FD, Cosgrove DM, Ratliff NB, Easley K, Taylor PC. Long-term (5 to 12 years) serial studies of internal mammary artery and saphenous vein coronary bypass grafts. J Thorac Cardiovasc Surg 1985; 89:248–58.

[4] Loop FD, Lytle BW, Cosgrove DM, Stewart RW, Goormastic M, Williams GW, Golding LA, Gill GC, Taylor PC, Sheldon WC, Proudfit WL. Influence of the internal-mammary artery graft on 10-year survival and other cardiac events. N Engl J Med 1986;314:1–6.

[5] Zeff RH, Kongtahworn C, Iannone LA, Gordon DF, Brown TM, Phillips SJ, Skinner JR, Spector M. Internal mammary artery versus saphenous vein graft to the left anterior descending coronary artery: prospective randomized study with 10-year follow-up. Ann Thorac Surg 1988;45:533–6.

[6] Boylan MJ, Lytle BW, Loop FD, Taylor PC, Borsh JA, Goormastic M, Cosgrove DM. Surgical treatment of isolated left anterior descending coronary stenosis: comparison of left internal mammary artery and venous autograft at 18 to 20 years of follow-up. J Thorac Cardiovasc Surg 1994;107:657–62.

[7] Cameron AA, Green GE, Brogno DA, Thornton J. Internal thoracic artery grafts: 20-year clinical follow-up. J Am Coll Cardiol 1995;25:188–92.

[8] Cameron A, Davis KB, Green G, Schaff HV. Coronary bypass surgery with internal-thoracic-artery grafts-effects on survival over a 15-year period. N Engl J Med 1996;334(4):216–20.

[9] Barner HB. Double internal mammary-coronary artery bypass. Arch Surg 1974;109:627–30.

[10] Hashimoto H, Isshiki T, Ikari Y, Hara K, Saeki F, Tamura T, Yamaguchi T, Suma H. Effects of competitive flow on arterial graft patency and diameter: medium-term postoperative follow-up. J Thorac Cardiovasc Surg 1996;111:399–407.

[11] Seki T, Kitamura S, Kawachi K, Morita R, Kawata T, Mizuguchi K, Hasegawa J, Kameda Y, Yoshida Y. A quantitative study of postoperative luminal narrowing of the internal thoracic artery graft in coronary artery bypass surgery. J Thorac Cardiovasc Surg 1992;104:1532–8.

[12] Siebenmann R, Egloff L, Hirzel H, Rothlin M, Studer M, Tartini R. The internal mammary artery "string phenomenon." Analysis of 10 cases. Eur J Cardiothorac Surg 1993;7:235–8.

[13] Kawasuji M, Tedoriya T, Takemura H, Sakakibara N, Taki J, Watanabe Y. Flow capacities of arterial grafts for coronary artery bypass grafting. Ann Thorac Surg 1993;56:957–62.

[14] Kobayashi J, Tagusari O, Bando K, Niwaya K, Nakajima H, Ishida M, Fukushima S, Kitamura S. Total arterial off-pump coronary revascularization with only internal thoracic artery and composite radial artery grafts. Heart Surg Forum 2002;6:30–7.
[15] Nakajima H, Kobayashi J, Tagusari O, Bando K, Niwaya K, Kitamura S. Functional angiographic evaluation of individual, sequential, and composite arterial grafts. Ann Thorac Surg 2006;81:807–14.
[16] Nakajima H, Kobayashi J, Tagusari O, Niwaya K, Funatsu T, Kawamura A, Yagihara T, Kitamura S. Angiographic flow grading and graft arrangement of arterial conduits. J Thorac Cardiovasc Surg 2006;132:1023–9.
[17] Schmidt SE, Jones JW, Thornby JI, Miller CC, Beall AC. Improved survival with multiple left-sided bilateral internal thoracic artery grafts. Ann Thorac Surg 1997;64:9–14.
[18] Campeau L, Enjalbert M, Lespérance J, Vaislic C, Grondin CM, Bourassa MG. Atherosclerosis and late closure of aortocoronary saphenous vein grafts: sequential angiographic studies at 2 weeks, 1 year, 5 to 7 years, and 10 to 12 years after surgery. Circulation 1983;68:II1–7.
[19] Dion R, Glineur D, Derouck D, Verhelst R, Noirhomme P, El Khoury G, Degrave E, Hanet C. Long-term clinical and angiographic follow-up of sequential internal thoracic artery grafting. Eur J Cardiothoracic Surg 2000;17:407–14.
[20] Dincer B, Barner HB. The "occluded" internal mammary artery graft: Restoration of patency after apparent occlusion associated with progression of coronary disease. J Thorac Cardiovasc Surg 1983;85:318–20.
[21] Aris A, Borrás X, Ramió J. Patency of internal mammary artery grafts in no-flow situations. J Thorac Cardiovasc Surg 1987;93:62–4.